



Research article

Early properties of magnesium phosphate cement repairing material used in slab track

Ji Wang^a, Liang Gao^{a,b,*}, Yanrong Zhang^{a,b}, Ludong Wang^a, Chenyu Xu^a^a School of Civil Engineering, Beijing Jiaotong University, Beijing, 100044, China^b Frontiers Science Center for Smart High-speed Railway System, Beijing, 100044, China

ARTICLE INFO

Keywords:

Ballastless track repair
Magnesium phosphate cement (MPC)
Central composite design (CCD)
Response surface methodology (RSM)
Early properties optimization

ABSTRACT

Magnesium phosphate cement (MPC) is a high-performance repairing material suitable for the interfacial disease of slab track. In this study, the early properties of MPC were optimized using central composite design (CCD) approach based on response surface methodology (RSM). Three factors with five levels and three responses were considered. The significance of the factors and their interactions were verified by using analysis of variance (ANOVA). The result show that the mass ratio of water-to-binder (W/b) affects fluidity, while the mass ratio of magnesia-to-phosphate (M/P) and borax-to-magnesia (B/M) impact the setting time of MPC. Higher W/b results in higher fluidity, while an increase in M/P reduces the setting time by increasing the neutralization reaction. Borax addition retards the reaction, prolonging the setting time. The three factors significantly affect the early compressive strength of MPC. At M/P = 3.5, the interweaving of MgO and K-struvite (MKP) forms a dense network structure, enhancing the strength. Borax and W/b interact to affect compressive strength, with borax retarding MKP crystal growth and higher W/b reducing compactness. Combined with microscopic property test, the strength generation mechanism of MPC with optimized mixing ratio was revealed, And the feasibility of field application of MPC was verified by strength test.

1. Introduction

China's high-speed railway has developed rapidly, exceeding 45,000 km by the end of 2023. As an important structural form of high-speed railway, ballastless track has advantages such as strong integrity, high smoothness, and low maintenance workload [1,2]. With increasing service life, ballastless track has developed diseases such as the peeling, cracking and gapping, as shown in Fig. 1(a) and (b), respectively, which seriously affect the integrity of the track and the safe and high-speed operation of trains. Therefore, timely maintenance is required.

There are several studies [3–5], mainly on the properties of ballastless track repair materials, repair methods, and static and dynamic response of track structures before and after repair. The repair materials used mainly include organic repair materials represented by epoxy resin, silicone resin and polyurethane, and cement-based repair materials represented by cement mortar and asphalt mortar [3,6–8]. These materials can meet the performance requirements of repair materials in the current specifications, but they have different characteristics in terms of cooperating with the track structure for deformation, durability, secondary reparability, and environmental protection. Therefore, it is essential to propose a material with superior performance for the repair of diseases in

* Corresponding author. School of Civil Engineering, Beijing Jiaotong University, Beijing, 100044, China.
E-mail address: lgao@bjtu.edu.cn (L. Gao).

<https://doi.org/10.1016/j.heliyon.2024.e28913>

Received 31 October 2023; Received in revised form 13 March 2024; Accepted 26 March 2024

Available online 28 March 2024

2405-8440/© 2024 Published by Elsevier Ltd.

This is an open access article under the CC BY-NC-ND license

(<http://creativecommons.org/licenses/by-nc-nd/4.0/>).

ballastless track structures. At present, as a new type of rapid repair material, magnesium phosphate cement (MPC) has attracted attention. It has many advantages, such as short setting time, good flowability, high bond strength with concrete, and good secondary repairability [9–13]. In particular, MPC is an inorganic material with properties that are very close to those of the concrete used in the track structure. The repaired structure can deform synergistically under external loads to maintain the integrity of the structure. MPC repair materials have been widely used in many fields such as housing, bridge and road maintenance [13–15], but has not been widely used in the track field. Several researchers have studied the feasibility of using MPC to maintain track structures. Chen [16] established a finite element model to study the stress-strain characteristics of MPC-repaired ballastless tracks under different temperature conditions, and the results showed that MPC is more suitable than epoxy resin for the repair of slab track crack disease. Xu [4] obtained the cohesive parameters between MPC and concrete through experiments and established a CRTS II slab track repair model, and the results showed that the repaired MPC-track interface had good bonding performance under temperature loading. Jiang [17] investigated the mechanical properties of the repaired ballastless track base plate of MPC-concrete composite specimens through flexural and fatigue bending tests, and it was demonstrated that MPC can quickly restore the structural performance, and the repaired specimens show stronger fatigue performance. The above literature indicates that MPC has excellent performance and great potential in the repair of ballastless track. However, the previous studies mainly focused on the mechanical properties of the repaired track structure after using MPC, and less attention was paid to the influence of MPC properties on the convenience of repair construction. Since the repair of ballastless track is generally carried out during the maintenance window, the performance requirements for repair materials, such as fluidity, setting time and early strength, are relatively high. Therefore, in order to promote the application of MPC in high-speed railway, it is crucial to optimize the early properties of MPC taking into account the characteristics of ballastless track maintenance.

Currently, the early performance of MPC has been studied by some researchers. Qiao and Li [18,19] found that increasing the mass ratio of magnesia-to-phosphate (M/P) can shorten the setting time of MPC, and the strength of MPC mortar increases first and then decreases with the increase of M/P. Li [20] found that increasing the mass ratio of water-to-binder (W/b) can significantly prolong the setting time, and the higher the W/b, the lower the early compressive strength. Hou [21] found that increasing the M/P could shorten the setting time and decrease the early compressive strength of MPC. The above research mainly investigated the variation law of the early performance of MPC by changing the basic mixing ratio, and some researchers studied the effect of different additives on the early performance of MPC. Liu [22] investigated the effect of ground granulated blast furnace slag (GGBS) on the properties of MPC and found that GGBS significantly shortened the setting time, improved the fluidity, and enhanced the mechanical properties of the samples. Xu [23] studied the effect of silica fume on the properties of MPC and found that appropriate addition of silica fume can increase the fluidity, extend the setting time, and improve the early compressive strength of MPC. Tan [24] studied the effect of polycarboxylate superplasticizer (PCE) on the fluidity of MPC and found that the addition of PCE can improve the fluidity of MPC by slowing down the hydration process. Dong [25] found that the addition of spherical fly ash can improve the fluidity of magnesium ammonium phosphate cement (MAPC) and extend the setting time. Wu [26] added metakaolin to MPC and found that metakaolin has a high activity that can react with phosphate to form aluminum phosphate gel, which fills the pores between crystals and improves early compressive strength. Liu [27] investigated the properties of MPC after the addition of nano-silica and found that within a certain range of addition, the fluidity decreased, the setting time shortened, and the early compressive strength increased. The above research is mainly based on adjusting the basic mixing ratio of material or selecting different kinds of admixtures as a method to obtain the influence of single factors such as the ratio parameters or admixture dosage on an early performance of MPC by conducting a large number of experiments, and then get a better mixing ratio. However, the mixing ratio obtained by this method has certain limitations. It cannot reveal the influence of multi-factor interactions in the system and is not optimal in a mathematical sense. Therefore, it is necessary to select a design method for mixing ratio optimization that is adaptable to the interactions of multiple factors in the system.

Response Surface Methodology (RSM) is an optimization method that integrates experimental design and mathematical modeling. It helps understand the interactions among the factors to be optimized while reducing the number of experiments. Central Composite Design (CCD), as the primary design method in RSM, has been widely used in fields such as pharmaceuticals, agriculture, and chemical engineering [28–31]. This method conducts experiments at representative points to regression fit the functional relationship between each factor and the response value, and then accurately predicts the optimal experimental design. Currently, there is limited research on optimizing the MPC ratio using the CCD method. Hou [32] optimized the mixing ratio of MPC based on the CCD method, with setting time and high compressive strength as targets, and applied it to concrete pavement repair. Yue [33] studied the effects of W/b, M/P, and borax on the rheological properties of MPC based on the CCD method, and optimized the mixing ratio to improve the rheological properties. Some researchers used the CCD method for the optimization of the mixing ratio of ordinary Portland cement,

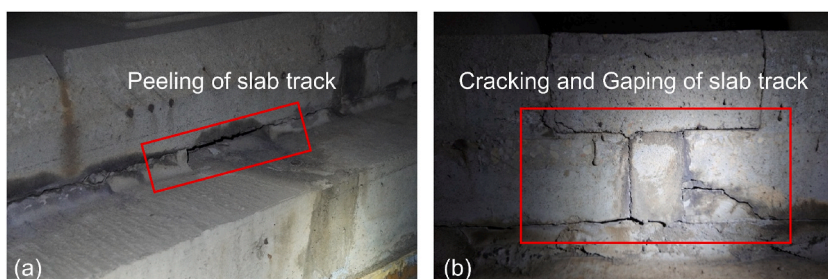


Fig. 1. Typical diseases of ballastless track on high-speed railways.

which can also provide references for this study. Aldahdooh [34] optimized the dosage of Portland cement and silica fume based on the CCD method to achieve higher strength in fiber-reinforced concrete. Rooholamini [35] studied the effects of fibers, cement, and water on the strength of roller-compacted concrete based on the CCD method to provide guidance for the design of high-performance pavements. Awolusi [36] predicted and optimized the properties of concrete containing steel fibers extracted from waste tires with limestone powder as filler based on the CCD method, and the results showed that the proposed mathematical model could predict the required properties of fiber-reinforced concrete for early decision-making during construction. It can be seen that the current research on the optimization of the mixing ratio of MPC using the CCD method is relatively limited, and a large number of studies focus on optimizing the mixing ratio of ordinary Portland cement. The mathematical model constructed using the CCD method can accurately determine the effect of multiple factors on the properties of cementitious materials and obtain the optimal mixing ratio under target properties requirements. Therefore, it is feasible to use the CCD method to optimize the MPC mixing ratio with the aim of repairing ballastless track disease.

MPC is a high-performance inorganic rapid repair material that is well-suited for repairing ballastless track diseases. By optimizing the mixing ratio, the workability and mechanical properties of MPC can be improved to match the performance requirements of ballastless track repair materials. In this paper, aiming at the repair construction of ballastless track, the influence law of M/P, W/b and borax content on the fluidity, setting time and early compressive strength of MPC were studied. Based on the CCD method, the properties optimization model of MPC was constructed, and the significance and adequacy of the optimization model were evaluated by the analysis of variance (ANOVA). The mixing ratio of MPC suitable for ballastless track repair was obtained. On the basis of the optimized ratio, the evolution law and mechanism of compressive strength and bonding strength of MPC was studied, which provides theoretical support for the application of MPC in high-speed railway ballastless track maintenance.

2. Experimental

2.1. Raw materials

In this paper, the chemical composition of dead-burnt (1700 °C) MgO with a specific surface area of 2700 cm²/g and a purity of 95% provided by Weifang Dakang Chemical Co., Ltd., Shandong, China is shown in Table 1. Potassium dihydrogen phosphate (KH₂PO₄) with a purity of 97% and borax (Na₂B₄O₇·10H₂O) with a purity of 95% are provided by Tianjin Jinhuitaiya Chemical Reagent Co., Ltd., China. The chemical composition of fly ash with a specific surface area of 4300 cm²/g is shown in Table 2. Deionized water is used in the experiments.

2.2. Experimental design

In order to improve the accuracy and efficiency of experiments and to precisely design the high fluidity rapid repair materials, the CCD method in RSM was used to design the mixing ratio of the MPC.

2.2.1. Mix ratio design

In this paper, considering the main factors of the early properties of MPC, the mass ratio of magnesia-to-phosphate (x_1 : M/P), the mass ratio of borax to magnesia (x_2 : B/M) and the mass ratio of water to binder (x_3 : W/b) are selected as the input factors of the optimization model. Some scholars have investigated the property of MPC under different mixing ratios and found that when the M/P falls within the range of 3–4 [19,37], the B/M is approximately 12.5% [38,39], and the W/b varies from 0.14 to 0.2 [40,41], the individual properties of MPC are closely with the requirements for the slab track repair. Consequently, this study broadens the range of each factor, setting the ranges for M/P, B/M, and W/b as 2.7 to 4.3, 0.11 to 0.17, and 0.12 to 0.22, respectively, to ensure that the factor ranges cover the various property aspects of MPC. In order to match the property requirements of the repair material for ballastless track diseases, fluidity (y_1), setting time (y_2), and early compressive strength (y_3) are selected as response values. An experimental design with three factors and five levels is designed on the basis of the CCD method, which involves 2^k cube points, 2k star points, and n center points [33]. Among them, k and n represent the number of factors and the number of repetitions of the center point, respectively. In this paper, k and n are 3 and 5, respectively, so there are 8 cube points, 6 star points and 5 center points (as shown in Fig. 2). Based on the results of preliminary experiments, the range and code values of each factor are shown in Table 3. Furthermore, 19 groups experimental mixing designs of the MPC are obtained.

According to the designed mixing ratio combined with Fig. 2, MP-01 to MP-08 (Green dots) are cube points, located at the corners of the cube, with coded values of 1 or -1, mainly used to evaluate the interaction and linear terms among factors. MP-09 to MP-14 (Yellow dots) are star points, with coded values of 1.682 or -1.682, which are used primarily for evaluation of nonlinear relationships among factors. MP-15 to MP-19 (Red dots) are center points, located in the center of the cube with coded values of 0, mainly used to reduce the deviation of the regression coefficient and improve the accuracy of the regression model. Furthermore, several studies

Table 1
Chemical compositions of MgO.

Component	MgO	SiO ₂	CaO	Fe ₂ O ₃	Al ₂ O ₃	Others
Content (%)	95.56	1.28	1.86	0.72	0.10	0.48

Table 2
Chemical compositions of fly ash.

Component	SiO ₂	CaO	Fe ₂ O ₃	Al ₂ O ₃	K ₂ O	Na ₂ O	SO ₃	TiO ₂	MgO	Others
Content (%)	47.84	4.81	5.12	30.43	1.50	0.42	1.33	1.63	0.50	6.42

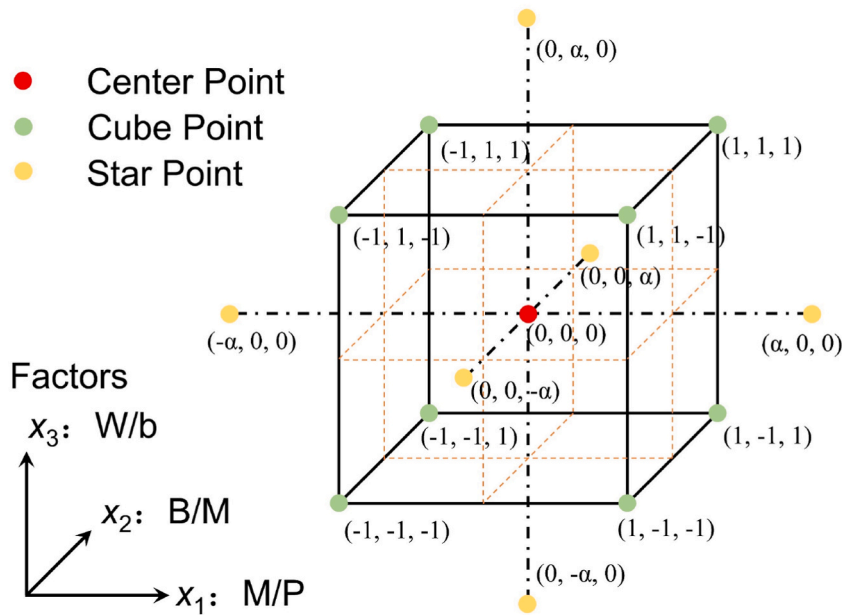


Fig. 2. Schematic of experiment points with coded values.

Table 3
Comparison of factor values and coding values.

Factors	Coded levels				
	$-\alpha$	-1	0	1	α
x_1 : M/P	2.7	3	3.5	4	4.3
x_2 : B/M	0.11	0.12	0.14	0.16	0.17
x_3 : W/b	0.12	0.14	0.17	0.2	0.22

Notes: $\alpha = (2^k)^{\frac{1}{4}} = 1.682$.

have indicated that the addition of an appropriate amount of fly ash can improve the workability and mechanical properties of the MPC paste. This enhancement is primarily attributed to the spherical shape of fly ash particles, which enhances the fluidity of the paste. Additionally, due to its inert chemical reaction, fly ash can extend the setting time. Simultaneously, it contributes to densifying the microstructure of the MPC paste, consequently increasing its mechanical strength. Moreover, the incorporation of fly ash can lead to cost savings, thereby reducing the overall price of MPC [42–44]. Therefore, 10 wt% fly ash was added to the MPC in this study.

2.2.2. Sample preparation

The MPC paste samples were prepared according to the mixing ratio mentioned in section 2.2.1, using the following procedure: First, the weighed dry powders including MgO, KH₂PO₄ (KDP), borax, and fly ash are added to the mixing bowl and stirred for 60 s. Then add water and stir at low speed for 60 s, then at high speed for 60 s. Finally let stand for 30 s to obtain the uniform MPC paste. For the fluidity and setting time tests, the freshly mixed paste was used directly. For the strength test, the specimens were cured under dry conditions (20 °C and 65% RH) to the specified age before testing.

2.3. Test methods

2.3.1. Fluidity and setting time test

Test the fluidity and setting time of the fresh MPC paste. For fluidity, the test method follows the Chinese standard GB/T 8077-2012. The truncated cone mold filled with fresh MPC paste is lifted vertically. The maximum diameter of the paste is measured in two directions perpendicular to each other, and the average is taken as its fluidity. The setting time is tested in accordance with Chinese standard GB/T 1346-2011. A needle is dropped every 30 s during the test and every 15 s when it is close to setting. It is worth noting that the setting process of MPC is faster than that of ordinary Portland cement, and the time interval between initial and final setting is very short. Therefore, its initial setting time is mainly tested and it is used to represent its setting time in this paper [23].

2.3.2. Compressive and bonding strength

Mechanical property testing of MPC specimens includes compressive strength and bond strength. The compressive strength test method refers to the Chinese standard GB/T 17671-2021. The specimen size is 40 mm 40mm × 40 mm and is cured under dry curing conditions (20 °C and 65% RH) for 4 h. Six specimens are tested in each group, and the arithmetic mean of the six test results is taken as the result for the group. The test method for bonding strength refers to JC/T 2537-2019. Portland cement mortar of 80 mm × 40 mm × 40 mm was prepared in advance and cured for 28 days, and then the freshly mixed MPC paste and cement mortar block were co-molded to form a bonding strength test specimen. The flexural strength of the specimen represents the bonding strength. Each test group contains 3 specimens and the arithmetic mean of the results of 3 tests is taken as the result of the group. It should be noted that the early compressive strength of all groups is tested in this paper. It is because early compressive strength is an important indicator of the repair material for ballastless track, which will guide the establishment of the regression model and the optimization of the mixing ratio. In addition, to further understand the evolution law of the mechanical properties of MPC after the mixing ratio optimization, it is necessary to test the compressive strength and bonding strength at 4h, 12h, 1d, 3d, 7d, 14d, and 28d.

2.3.3. SEM and EDS

This paper examines the microscopic morphology and pore structure of MPC to understand its microscopic properties. In the testing process, the remaining blocks used for early compressive strength testing were cut into specimens measuring about 10 mm × 10 mm × 5 mm. Next, the samples were soaked in an alcohol bath for 24 h and dried in a vacuum oven for 48 h to ensure timely removal of water from the MPC paste and termination of hydration reaction. Afterwards, some samples were coated with a thin film of gold and observed using SEM (Phenom ProX) to analyze the microstructure. Corresponding points were also analyzed by EDS technology for elemental analysis.

3. Results and discussion

3.1. Effects of the variables on fluidity

ANOVA is used to evaluate the interaction among each analyzed factor, with a p-value of less than 0.05 indicating a significant effect of the analyzed factor [29]. Table 4 shows that x_1 : M/P, x_2 : B/M, and x_3 : W/b significantly affect the fluidity of MPC, and there is a strong linear relationship between fluidity (y_1) and the three factors (x_1, x_2, x_3). The resulting equation after linear fitting is shown in equation (1):

$$y_1 = -26.15381x_1 + 462.31365x_2 + 1163.35495x_3 + 29.57179 \tag{1}$$

According to the ANOVA analysis, the p-value of the regression model is less than 0.0001, which suggests that the model has high statistical significance. The coefficient of determination (R^2) of the model is 0.9489, indicating that more than 94.9% of the changes in the response value are related to the three independent factors, and the low coefficient of variation (C.V.) also confirms this. Furthermore, the adjusted correlation coefficient (Adj- R^2) is strongly correlated and in a logical agreement with the prediction

Table 4
ANOVA statistics of the regression equation of fluidity and setting time.

Source	d_f	Mean square		F-value		p-value	
		y_1	y_2	y_1	y_2	y_1	y_2
Model	3	6712.57	25521.76	92.8	110.09	<0.0001	<0.0001
x_1 : M/P	1	2335.4	30548.25	32.29	131.77	<0.0001	<0.0001
x_2 : B/M	1	1167.52	29910.94	16.14	129.02	0.0011	<0.0001
x_3 : W/b	1	16634.8	16106.08	229.97	69.48	<0.0001	<0.0001
Residual	15	72.33	231.82	–	–	–	–
Lack of fit	11	85.62	285.47	2.39	3.39	0.2076	0.125
Pure error	4	35.8	84.3	–	–	–	–
	R^2	Adj- R^2		Pred- R^2		C.V.(%)	
y_1	0.9489	0.9386		0.9134		4.24	
y_2	0.9566	0.9479		0.9314		2.03	

correlation coefficient (Pred-R²), which is significantly less than the requirement in the statistical recommendation that the difference between these two values is less than 20% [45], indicating that the predicted values of the model are in good agreement with the experimental values. The p-value of the lack-of-fit is greater than 0.05, indicating that it can be ignored. Thus, the established regression model is reasonable and effective. Based on this, the independent and interactive effects of the three factors on fluidity were extracted, as shown in Fig. 3.

From Fig. 3(a), it is apparent that within the range of mixing ratio, W/b is the factor that determines the fluidity, while the effect of M/P and B/M are relatively small. The interaction effects of the variables on the fluidity are shown in Fig. 3(b) ~ Fig. 3(d), respectively. Specifically, the increase of W/b significantly increases fluidity. This can be attributed to the decrease in the proportion of solid phase and the increase in particle distance, which leads to weakened interaction forces and reduced resistance to particle movement. The fluidity decreases with the increase of M/P. As the M/P ratio increases, the fluidity decreases. This is due to the increase in the amount of undissolved MgO particles in the paste, which causes the particle spacing to decrease and the resistance to particle movement to increase, resulting in a decrease in fluidity. The fluidity gradually increases with the increase of B/M. This is due to the dissolution of borax in water, which results in an alkaline solution that accelerates the dissolution of phosphate. The system absorbs heat, which reduces the rate of hydration reaction and inhibits the dissolution rate of MgO. This, in turn, increases the proportion of the liquid phase in the solution, and the release of 10 crystal water molecules after borax dissolution further increases the proportion of the liquid phase. These combined effects lead to an increase in the fluidity of the paste.

3.2. Effects of the variables on setting time

Table 4 shows that M/P, B/M, and W/b have a significant effect on the setting time of MPC. Similar to the fluidity regression model, there is a strong linear relationship between the setting time (y₂) and the three factors, and the fitted equation is shown in equation (2):

$$y_2 = -94.59057x_1 + 2339.9666x_2 + 1144.71752x_3 + 560.44861 \tag{2}$$

According to the ANOVA, the p-value of the regression model is less than 0.0001, which indicates that the model has high statistical significance. The R² of the model is 0.9566, indicating that more than 95.7% of the variation in the response value is related to the three independent factors. In addition, the C.V. value, Pred-R², Adj-R², and p-value of lack of fit all indicate that the established regression model is reasonable and effective. Furthermore, the independent and coupling effect of the three factors on setting time

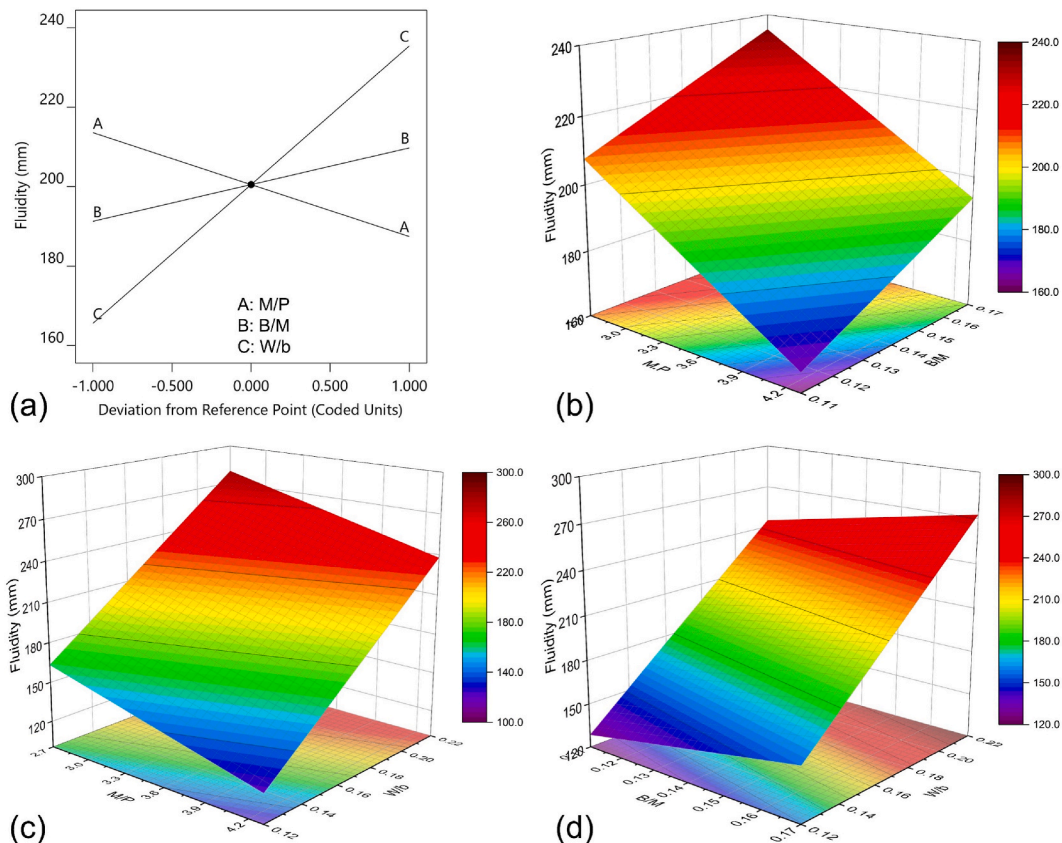


Fig. 3. Effects of the variables on fluidity.

were extracted, as shown in Fig. 4.

From Fig. 4(a), it can be seen that the effect of each factor on the setting time is significant within the mixing ratio range. M/P and B/M have similar but opposite effects on the setting time. The effect of W/b on the setting time is relatively weak. The interaction effects of the variables on the setting time are shown in Fig. 4(b) ~ Fig. 4 (d), respectively. More precisely, the setting time decreases with the increase of M/P. This is mainly due to the increased amount of $Mg(OH)_2$ dissolved in the paste, which leads to more intense neutralization reactions with KDP. Consequently, the rate and amount of the hydration product MKP also increase, accelerating the setting of the paste. The setting time increases with higher B/M. Borax dissolution produces $B_4O_7^{2-}$ which easily combines with Mg^{2+} from MgO dissolution, hindering the reaction between Mg^{2+} and $H_2PO_4^-$. Meanwhile, the product of the combination easily adsorbs on the surface of MgO to form a film, and hinder the dissolution of MgO. Both factors together delay the paste setting process. As the W/b increases, the setting time is prolonged. This is because the relatively higher water content reduces the temperature of the paste and decelerates the reaction rate of Mg^{2+} and $H_2PO_4^-$, thereby delaying the setting process of the paste.

3.3. Effects of the Variables on Compressive Strength

The significant test results for the early compressive strength regression model are presented in Table 5. The table shows that the three independent factors, M/P, B/M, and W/b, significantly affect the early compressive strength of MPC. Furthermore, the ANOVA shows that the quadratic terms x_1^2 , x_2^2 , x_3^2 , and the interaction term $x_2 x_3$ also have a significant effect on the early compressive strength. The regression equation between the compressive strength (y_3) and the factors is obtained by least squares analysis, as shown in equation (3):

$$y_3 = -3.79354x_1^2 - 2238.37888x_2^2 + 988.9923x_3^2 - 23.5x_1x_2 - 17.16667x_1x_3 + 2300x_2x_3 + 34.99427x_1 + 46.49912x_2 - 741.16491x_3 + 40.98246 \tag{3}$$

It can be seen from Table 5 that the p-value of the model is less than 0.0001, indicating high statistical significance. The R^2 and C.V. values are 0.9883 and 6.72%, respectively, suggesting a good correlation between the model and the independent factors. In addition, the $Pred-R^2$, $Adj-R^2$, and p-values of the lack-of-fit terms indicate that the established regression model is reasonable and effective. The

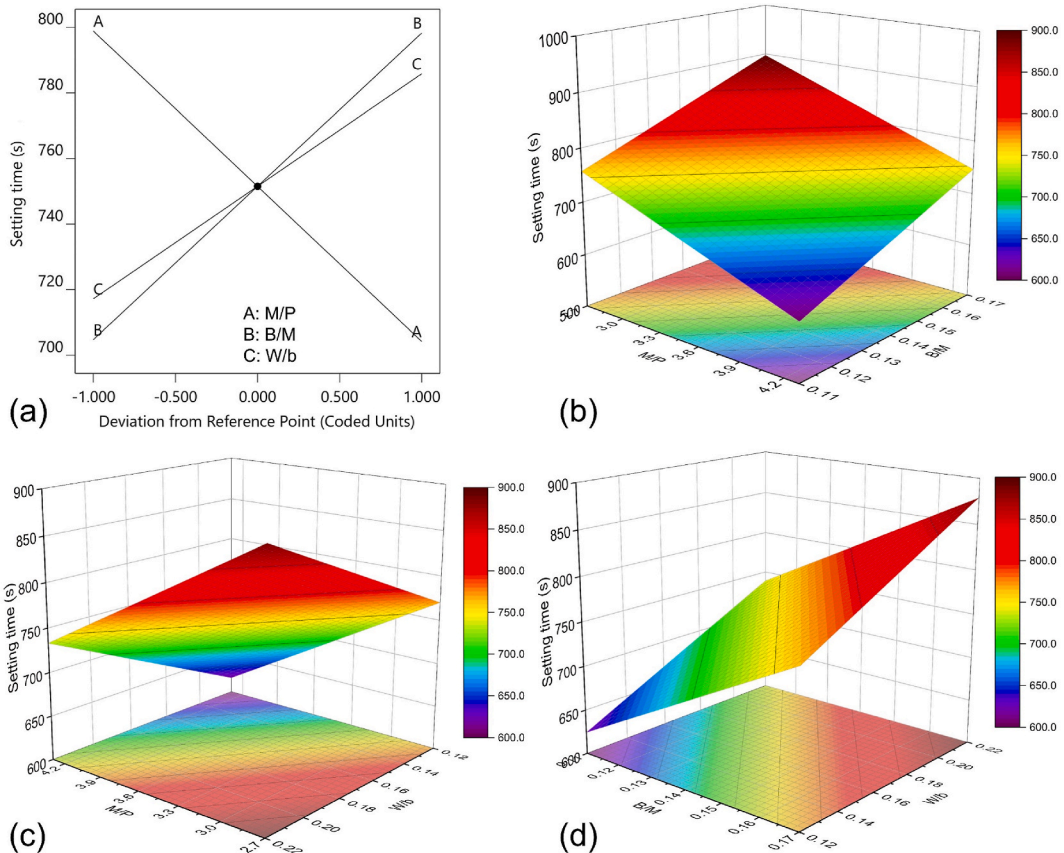


Fig. 4. Effects of the Variables on setting time.

Table 5
ANOVA statistics of the regression equation of compressive strength.

Source	d_f	Mean square	F-value	p-value
Model	9	80.6	84.53	<0.0001
x_1 : M/P	1	17	17.83	0.0022
x_2 : B/M	1	402.66	422.31	<0.0001
x_3 : W/b	1	251.31	263.57	<0.0001
$x_1 x_2$	1	0.4418	0.4634	0.5132
$x_1 x_3$	1	0.5304	0.5563	0.4748
$x_2 x_3$	1	15.24	15.98	0.0031
x_1^2	1	12.28	12.88	0.0059
x_2^2	1	10.94	11.48	0.008
x_3^2	1	10.81	11.34	0.0083
Residual	9	0.9535	–	–
Lack of fit	5	1.06	1.3	0.4104
Pure error	4	0.816	–	–
Cor total	18	–	–	–
R^2	Adj- R^2	Pred- R^2	C.V.(%)	–
0.9883	0.9766	0.9381	6.72	–

effect of each factor on the early compressive strength is shown in Fig. 5.

From Fig. 5(a), it can be seen that the early compressive strength is significantly affected by three factors, with $B/M > W/b > M/P$ as the order of importance. All three factors show obvious non-linear characteristics. The effect of B/M and W/b on early compressive strength is relatively close, while the effect of M/P is relatively small. The interaction effects of the variables on the compressive strength are shown in Fig. 5 (b) ~ Fig. 5 (d), respectively. Specifically, regardless of the changes in B/M and W/b, as M/P increases, the early compressive strength first increases and then decreases. When $M/P = 3.5$, the strength is relatively high. At this time, the hydration product K-struvite (MKP) envelops the unreacted MgO, resulting in the formation of a relatively dense network structure [46]. When M/P is low, the paste is dominated by MKP and relatively low MgO. In addition, unreacted phosphates are still present,

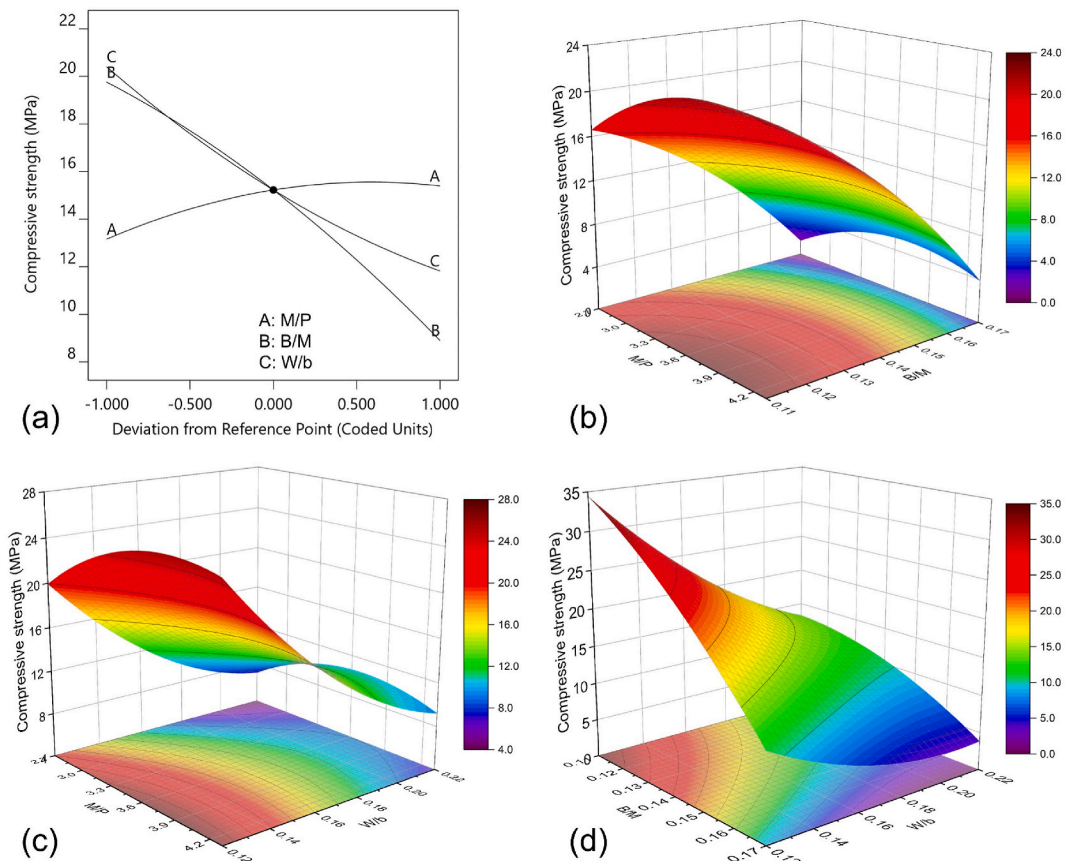


Fig. 5. Effects of the variables on compressive strength.

preventing the development of strength and the formation of a denser network structure. On the other hand, when M/P is high, there is more unreacted MgO and limited MKP, which cannot form a stable network structure, which also affects the development of strength. Increasing B/M results in a significant reduction in early compressive strength. The interaction between M/P and B/M is not significant, while the interaction between W/b and B/M is more evident. At low W/b, the sensitivity of early strength to B/M is strong, whereas it is relatively weak at high W/b. This is because the early strength of MPC has already decreased significantly at high W/b, so increasing B/M will not cause a significant decrease in strength. As the W/b increases, the early strength of MPC decreases significantly. This is because the water content in the paste increases as the W/b increases. As the reaction progresses, water is continuously consumed, resulting in an increase in pore content and a decrease in compactness, which ultimately leads to a decrease in strength. Overall, the three factors strongly interact to affect the early compressive strength of MPC, which is also confirmed by the results in Table 5. In this study, the influence laws and mechanisms of each factor on early strength are investigated. As early strength is one of the most important performance indicators of ballastless track rapid repair materials, it should be adequately addressed. To determine the material mixing ratio applicable to rapid repair construction, the optimization design of the mixing ratio needs to be discussed.

3.4. Optimization design of mix ratio

To develop high-performance MPC suitable for repairing ballastless tracks gapping and peeling diseases, it is necessary to clarify the requirements of the material for the repair construction. The freshly mixed paste should have high fluidity to easily fill small spaces such as cracks and gaps, and it should have excellent and stable workability to allow personnel and equipment to work during the repair construction. The setting time of the repair material should be in the range of 10–15 min. High early strength is also required in the repair material to meet the needs of rapid repair of track structures during the window period. Based on the optimization target of the above conditions and the influence laws of the three factors on the MPC property, the mixing ratio of MPC was optimized and present in Table 6. It can be seen that the optimized mixing ratio of MPC is M/P = 3.5, B/M = 0.12, and W/b = 0.18. Furthermore, verification tests were conducted using the optimized mixing ratio to evaluate its accuracy, and the comparison between the predicted and experimental values is shown in Table 7.

From Tables 7 and it can be seen that the relative error between the experimental and predicted values is less than 10%, indicating that the regression model can well reflect the influence of various factors on property of MPC. Moreover, the experimental results meet the relevant indicators of early property of repair materials in TG/GW 115–2012. Moreover, the microscopic morphology of the early age MPC under the optimized mixing ratio was tested to reveal the strength generation mechanism, as shown in Fig. 6.

Fig. 6 shows that the microstructure of MPC consists of columnar crystals, irregular powdery substances, and spherical particles. In order to distinguish the products with different shapes, three spots with more obvious features were selected for EDS analysis as shown in Fig. 6(b)–Fig. 6 (c) and Fig. 6 (d). The results indicate that the irregular powdery substance at spot 1 is MgO, as it mainly contains Mg and O elements with a content of over 90%. The columnar crystals are the hydration product K-struvite (MKP), as spot 2 shows a content of Mg, K, and P elements of about 10%, with a ratio close to 1:1:1. The spherical particles at spot 3 contain a high content of O element, along with Si and Al, indicating that they are fly ash. Overall, it can be seen from Fig. 6(a) that the content of MKP and MgO produced by the reaction is roughly equal and uniformly distributed, forming a denser network structure, which further confirms the correctness of the analysis in Section 3.3. To further verify the feasibility of the optimized mixing ratio of MPC proposed for repair construction, in this paper, compressive strength tests of MPC at different ages were conducted to obtain the strength development law of MPC. Moreover, flexural strength tests of composite specimens of MPC-Portland cement mortar at different ages were conducted to demonstrate the bonding strength development law between MPC and cementitious materials. The test results are shown in Fig. 7.

It can be seen from Fig. 7(a) that the compressive strength of MPC increases rapidly during the first 3 days, stabilizes after 7 days, and peaks at 43.7 MPa after 28 days. Although the compressive strength is slightly lower than that in the Ref. [47], this situation is also reasonable due to the significantly stronger fluidity of the MPC prepared in this paper. At 4 h, the strength is 15.7 MPa, which meets the requirement of TG/GW 115–2012 that the early compressive strength of repair materials should exceed 15 MPa. Similarly, from Fig. 7 (b), the bonding strength between MPC and Portland cement mortar increases rapidly during the first 3 days, stabilizes after 7 days, and peaks at 4.07 MPa after 28 days. Compared with the bonding strength measured in the Ref. [12], the bonding strength between the optimized MPC and Portland cement mortar in this paper is about 9.1% higher. At 3 days, the bonding strength is 3.32 MPa, also meeting the requirement of TG/GW 115–2012 that the early bonding strength of repair materials should exceed 3 MPa. Therefore, the properties of MPC optimized by CCD method meet the requirements for repair construction, making MPC a new option for repairing ballastless track diseases of high-speed railways. The CCD method is also effective for developing new repair materials.

4. Conclusions

In this paper, an early property optimization model for MPC was established based on the CCD method in RSM. The individual and combined effects of three key factors, M/P, B/M, and W/b, on the fluidity, setting time, and early compressive strength were

Table 6
Optimization target and optimized mixing ratio of MPC.

Response	y_1 : fluidity	y_2 : setting time (s)	y_3 : compressive strength	Factor	x_1 : M/P	x_2 : B/M	x_3 : W/b
Target	maximize	600–900	maximize	Mixing ratio	3.5	0.12	0.18

Table 7
Comparison of predicted value and experimental value of MPC.

Response	Predicted value	Experimental value	ARD/%
y_1 : fluidity (mm)	207	215	3.86
y_2 : setting time (s)	720	650	9.72
y_3 : compressive strength (MPa)	17.3	15.7	9.25

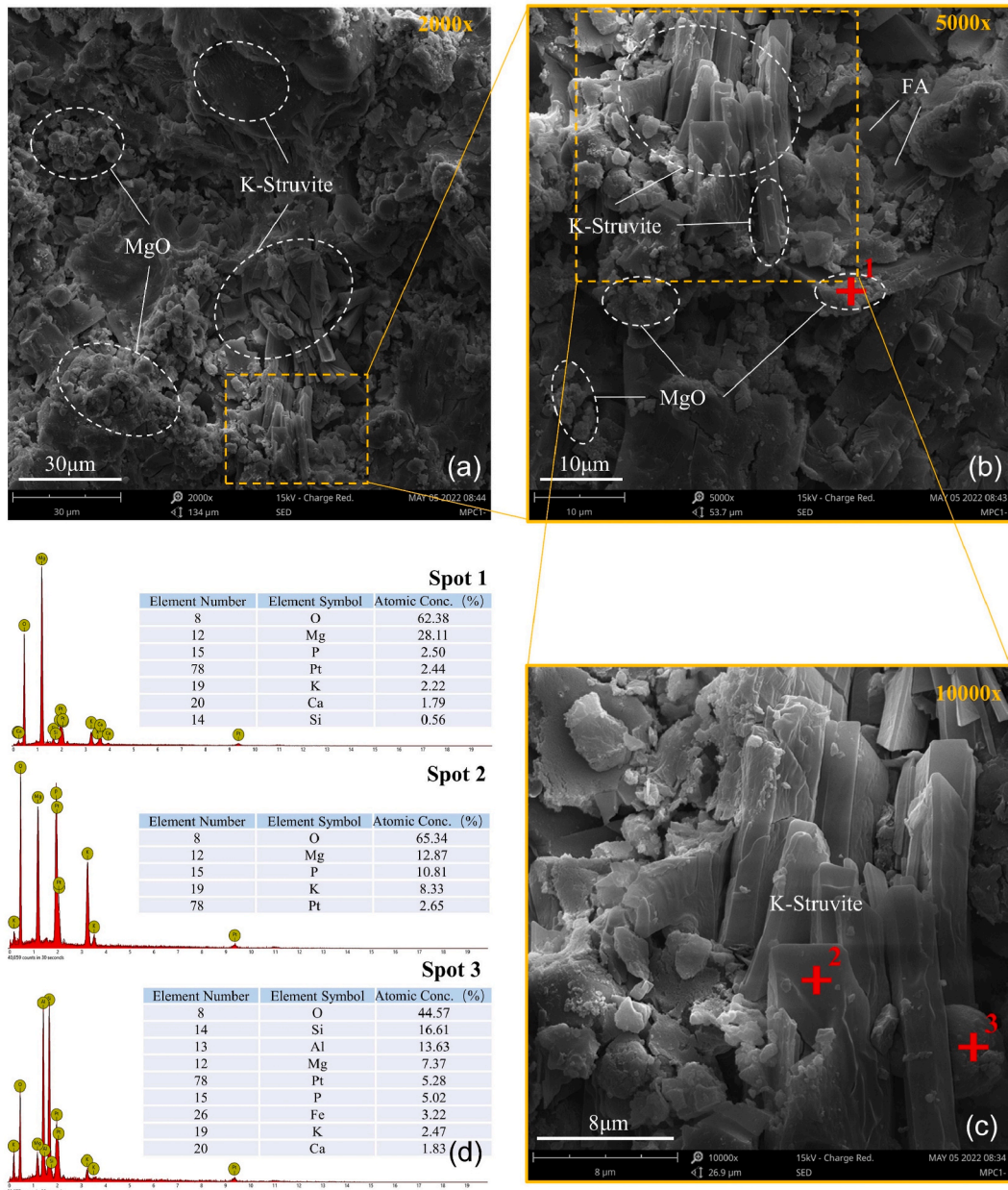


Fig. 6. SEM images of MPC under optimized mixing ratio and EDS analysis of the reaction products.

thoroughly investigated. Combined with the repair construction requirements for slab track diseases, the mixing ratio of MPC was optimized. The strength generation mechanism of MPC under optimized mixing ratio was revealed by microscopic property test. The feasibility of MPC in field application was verified by strength tests. The following conclusions can be drawn based on these results:

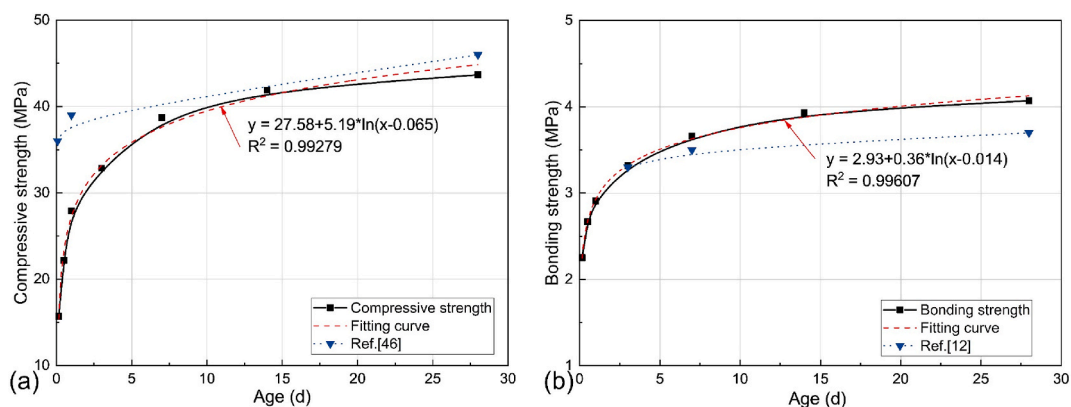


Fig. 7. Strength development law of MPC (a) Compressive strength; and (b) Bonding strength.

- (1) An optimization model for the early property of MPC was constructed based on the CCD method. In response to the repair needs of slab track defects in high-speed railways, the mixing ratio of MPC was optimized. The statistical analysis and equation validation results indicate that the CCD method is an effective approach for design optimization of MPC repair materials, which can obtain more accurate response equations while reducing the number of experiments.
- (2) For the workability of MPC, W/b is the main factor influencing the fluidity of MPC, which mainly changes the relative content of solid phase and particle spacing within the system to change the movement resistance between particles, with higher W/b results in higher fluidity. M/P and B/M primarily affect the setting time of MPC. Increasing M/P increases the degree of neutralization reaction, thereby reducing the setting time. The addition of borax can adsorb on the surface of reactants to retard the reaction and prolong the setting time. Moreover, experimental values show that the effects of the three factors on the fluidity and setting time of MPC are approximately linearly related.
- (3) The early compressive strength of MPC is significantly influenced by the three factors. M/P affects the content of MgO and MKP, which in turn affects the compressive strength. At M/P = 3.5, the interweaving of MgO and MKP forms a dense network structure, thereby increasing the strength of MPC, which can also be observed from SEM photos. B/M and W/b show a significant interaction effect, in particular, the addition of borax retards the crystal growth of MKP, while an increase in W/b increases the porosity of the cured paste, reducing the compactness and resulting in lower compressive strength of the MPC.
- (4) Aiming to repair the diseases of slab track in high-speed railway, the MPC obtained by the optimized mixing ratio fulfills the required material properties for repair including fluidity, setting time, compressive strength, and bonding strength. Moreover, both compressive strength and interfacial bonding strength showed a stable growth trend within 28 days. Therefore, MPC is a novel repair material option for ballastless track diseases in high-speed railways.

Data availability

Data will be made available on request.

CRediT authorship contribution statement

Ji Wang: Writing – original draft, Visualization, Data curation. **Liang Gao:** Supervision, Methodology, Funding acquisition, Conceptualization. **Yanrong Zhang:** Supervision, Resources. **Ludong Wang:** Writing – review & editing, Investigation. **Chenyu Xu:** Visualization, Writing – review & editing.

Declaration of competing interest

The authors declare that they have no known competing financial interests or personal relationships that could have appeared to influence the work reported in this paper.

Acknowledgment

This work was supported by the Fundamental Research Funds for the Central Universities (Science and technology leading talent team project, 2022JBQY009), the Fundamental Research Funds for the Central Universities (No. 2020JBZD013), the 111 Project (B20040), the Science and Technology Research and Development Project of China State Railway Group Co., Ltd. (P2021G053) and the Research Program of the Shandong Department of Transportation (2021B99).

References

- [1] J. Wang, L. Gao, W. Zhao, Y. Zhong, F. Tong, Q. Wang, Evolution mechanism of interlayer fatigue properties of CRTS III slab track, *Construct. Build. Mater.* 360 (2022) 129459, <https://doi.org/10.1016/j.conbuildmat.2022.129459>.
- [2] X. Cai, B. Luo, Y. Zhong, Y. Zhang, B. Hou, Arching mechanism of the slab joints in CRTSII slab track under high temperature conditions, *Eng. Fail. Anal.* 98 (2019) 95–108, <https://doi.org/10.1016/j.engfailanal.2019.01.076>.
- [3] Y. Zhang, K. Wu, X. Cai, L. Gao, K. Wang, X. Zhang, Numerical study on the pipe flow characteristics of grouting repairing pastes used in slab track, *Construct. Build. Mater.* 320 (2022) 126214, <https://doi.org/10.1016/j.conbuildmat.2021.126214>.
- [4] Y. Xu, D. Yan, W. Zhu, Y. Zhou, Study on the mechanical performance and interface damage of CRTS II slab track with debonding repairment, *Construct. Build. Mater.* 257 (2020) 119600, <https://doi.org/10.1016/j.conbuildmat.2020.119600>.
- [5] J. Ren, X. Li, R. Yang, P. Wang, P. Xie, Criteria for repairing damages of CA mortar for prefabricated framework-type slab track, *Construct. Build. Mater.* 110 (2016) 300–311, <https://doi.org/10.1016/j.conbuildmat.2016.02.036>.
- [6] H. Peng, Y. Zhang, J. Wang, Y. Liu, L. Gao, Interfacial bonding strength between cement asphalt mortar and concrete in slab track, *J. Mater. Civ. Eng.* 31 (7) (2019) 04019107, [https://doi.org/10.1061/\(ASCE\)MT.1943-5533.0002741](https://doi.org/10.1061/(ASCE)MT.1943-5533.0002741).
- [7] Y. Liu, F. Wang, M. Liu, S. Hu, A microstructural approach to adherence mechanism of cement and asphalt mortar (CA mortar) to repair materials, *Construct. Build. Mater.* 66 (2014) 125–131, <https://doi.org/10.1016/j.conbuildmat.2014.05.020>.
- [8] M.o.R.o.t.P.s.R.o. China, *Maintenance Rules for Ballastless Track of High-Speed Railway*, China Railway Publishing House Co., LTD., China, 2012.
- [9] N. Yang, C. Shi, J. Yang, Y. Chang, Research progresses in magnesium phosphate cement-based materials, *J. Mater. Civ. Eng.* 26 (10) (2014), [https://doi.org/10.1061/\(asce\)mt.1943-5533.0000971](https://doi.org/10.1061/(asce)mt.1943-5533.0000971).
- [10] J. Li, W. Zhang, Y. Cao, Laboratory evaluation of magnesium phosphate cement paste and mortar for rapid repair of cement concrete pavement, *Construct. Build. Mater.* 58 (2014) 122–128, <https://doi.org/10.1016/j.conbuildmat.2014.02.015>.
- [11] J. Qin, J. Qian, C. You, Y. Fan, Z. Li, H. Wang, Bond behavior and interfacial micro-characteristics of magnesium phosphate cement onto old concrete substrate, *Construct. Build. Mater.* 167 (2018) 166–176, <https://doi.org/10.1016/j.conbuildmat.2018.02.018>.
- [12] Y. Li, W. Bai, T. Shi, A study of the bonding performance of magnesium phosphate cement on mortar and concrete, *Construct. Build. Mater.* 142 (2017) 459–468, <https://doi.org/10.1016/j.conbuildmat.2017.03.090>.
- [13] M.A. Haque, B. Chen, Research progresses on magnesium phosphate cement: a review, *Construct. Build. Mater.* 211 (2019) 885–898, <https://doi.org/10.1016/j.conbuildmat.2019.03.304>.
- [14] L. Jun, J. Yongsheng, Z. Linglei, L. Benlin, W. Qing, D. Zuochao, Microstructure and property evolution of interfacial microregion of magnesium phosphate cement on mortar under various environments, *Struct. Concr.* 19 (4) (2018) 1122–1130, <https://doi.org/10.1002/suco.201700051>.
- [15] Q. Yang, B. Zhu, S. Zhang, X. Wu, Properties and applications of magnesium phosphate cement mortar for rapid repair of concrete, *Cement Concr. Res.* 30 (11) (2000) 1807–1813, [https://doi.org/10.1016/S0008-8846\(00\)00419-1](https://doi.org/10.1016/S0008-8846(00)00419-1).
- [16] B. Chen, S.Y. Oderji, S. Chandan, S. Fan, Feasibility of Magnesium Phosphate Cement (MPC) as a repair material for ballastless track slab, *Construct. Build. Mater.* 154 (2017) 270–274, <https://doi.org/10.1016/j.conbuildmat.2017.07.207>.
- [17] H. Jiang, J. Zhang, T. Li, Y. Wang, Y. Liu, H. De Backer, Feasibility analysis of magnesium phosphate cement as a repair material for base slab of China railway track system II ballastless track, *Construct. Build. Mater.* 326 (2022) 126821, <https://doi.org/10.1016/j.conbuildmat.2022.126821>.
- [18] F. Qiao, C. Chau, Z. Li, Property evaluation of magnesium phosphate cement mortar as patch repair material, *Construct. Build. Mater.* 24 (5) (2010) 695–700, <https://doi.org/10.1016/j.conbuildmat.2009.10.039>.
- [19] Y. Li, J. Sun, B. Chen, Experimental study of magnesia and M/P ratio influencing properties of magnesium phosphate cement, *Construct. Build. Mater.* 65 (2014) 177–183, <https://doi.org/10.1016/j.conbuildmat.2014.04.136>.
- [20] Y. Li, B. Chen, Factors that affect the properties of magnesium phosphate cement, *Construct. Build. Mater.* 47 (2013) 977–983, <https://doi.org/10.1016/j.conbuildmat.2013.05.103>.
- [21] D. Hou, H. Yan, J. Zhang, P. Wang, Z. Li, Experimental and computational investigation of magnesium phosphate cement mortar, *Construct. Build. Mater.* 112 (2016) 331–342, <https://doi.org/10.1016/j.conbuildmat.2016.02.200>.
- [22] Y. Liu, B. Chen, Research on the preparation and properties of a novel grouting material based on magnesium phosphate cement, *Construct. Build. Mater.* 214 (2019) 516–526, <https://doi.org/10.1016/j.conbuildmat.2019.04.158>.
- [23] X. Xu, X. Lin, X. Pan, T. Ji, Y. Liang, H. Zhang, Influence of silica fume on the setting time and mechanical properties of a new magnesium phosphate cement, *Construct. Build. Mater.* 235 (2020) 117544, <https://doi.org/10.1016/j.conbuildmat.2019.117544>.
- [24] H. Tan, X. Zhang, Y. Guo, B. Ma, S. Jian, X. He, Z. Zhi, X. Liu, Improvement in fluidity loss of magnesium phosphate cement by incorporating polycarboxylate superplasticizer, *Construct. Build. Mater.* 165 (2018) 887–897, <https://doi.org/10.1016/j.conbuildmat.2017.12.214>.
- [25] D. Dong, Y. Huang, Y. Pei, X. Zhang, N. Cui, P. Zhao, P. Hou, L. Lu, Effect of spherical silica fume and fly ash on the rheological property, fluidity, setting time, compressive strength, water resistance and drying shrinkage of magnesium ammonium phosphate cement, *J. Build. Eng.* 63 (2023) 105484, <https://doi.org/10.1016/j.jobe.2022.105484>.
- [26] Q. Wu, Y. Zou, J. Gu, J. Xu, R. Ji, G. Wang, The influence and action mechanization of mineral mixed material on high fluidity potassium magnesium phosphate cement (MKPC), *Journal of Composites Science* 4 (1) (2020) 29, <https://doi.org/10.3390/jcs4010029>.
- [27] Y. Liu, B. Chen, Z. Qin, Effect of nano-silica on properties and microstructures of magnesium phosphate cement, *Construct. Build. Mater.* 264 (2020) 120728, <https://doi.org/10.1016/j.conbuildmat.2020.120728>.
- [28] S. Bhattacharya, Central composite design for response surface methodology and its application in pharmacy, *Response surface methodology, engineering science*, IntechOpen (2021), <https://doi.org/10.5772/intechopen.95835>.
- [29] R. Ghelich, M.R. Jahannama, H. Abdizadeh, F.S. Torknik, M.R. Vaezi, Central composite design (CCD)-Response surface methodology (RSM) of effective electrospinning parameters on PVP-B-Hf hybrid nanofibrous composites for synthesis of HfB₂-based composite nanofibers, *Compos. B Eng.* 166 (2019) 527–541, <https://doi.org/10.1016/j.compositesb.2019.01.094>.
- [30] S. Sugashini, K.M.S. Begum, Optimization using central composite design (CCD) for the biosorption of Cr (VI) ions by cross linked chitosan carbonized rice husk (CCACR), *Clean Technol. Environ. Policy* 15 (2013) 293–302, <https://doi.org/10.1007/s10098-012-0512-3>.
- [31] Q. Zhang, X. Cai, K. Xie, Y. Zhang, Q. Wang, T. Wang, Multi-objective optimization for switch rail declining values of rail expansion joint on cable-stayed bridge, *Struct. Multidiscip. Optim.* 67 (3) (2024) 1–22, <https://doi.org/10.1007/s00158-023-03735-1>.
- [32] D. Hou, D. Chen, X. Wang, D. Wu, H. Ma, X. Hu, Y. Zhang, P. Wang, R. Yu, RSM-based modelling and optimization of magnesium phosphate cement-based rapid-repair materials, *Construct. Build. Mater.* 263 (2020), <https://doi.org/10.1016/j.conbuildmat.2020.120190>.
- [33] Y. Yue, J. Ren, K. Yang, D. Wang, J. Qian, Y. Bai, Investigation and optimisation of the rheological properties of magnesium potassium phosphate cement with response surface methodology, *Materials* 15 (19) (2022) 6815, <https://doi.org/10.3390/ma15196815>.
- [34] M. Aldahdooh, N.M. Bunnori, M.M. Johari, Evaluation of ultra-high-performance-fiber reinforced concrete binder content using the response surface method, *Mater. Des.* 52 (2013) 957–965, <https://doi.org/10.1016/j.matdes.2013.06.034>, 1980–2015.
- [35] H. Roololamini, A. Hassani, M. Aliha, Evaluating the effect of macro-synthetic fibre on the mechanical properties of roller-compacted concrete pavement using response surface methodology, *Construct. Build. Mater.* 159 (2018) 517–529, <https://doi.org/10.1016/j.conbuildmat.2017.11.002>.
- [36] T. Awolusi, O. Oke, O. Akinkulore, A. Sojobi, Application of response surface methodology: predicting and optimizing the properties of concrete containing steel fibre extracted from waste tires with limestone powder as filler, *Case Stud. Constr. Mater.* 10 (2019) e00212, <https://doi.org/10.1016/j.cscm.2018.e00212>.
- [37] W. Ibrahim, H. Sibak, M. Abadir, Preparation and characterization of chemically bonded phosphate ceramics (CBPC) for encapsulation of harmful waste, *The Journal of American Science* 7 (9) (2011) 543–548.

- [38] J. Yang, C. Qian, Effect of borax on hydration and hardening properties of magnesium and potassium phosphate cement pastes, *J. Wuhan Univ. Technol.-Materials Sci. Ed.* 25 (2010) 613–618.
- [39] J.B. Wen, L.X. Zhang, X.S. Tang, G.H. Huang, Y.R. Zhu, Effect of borax on properties of potassium magnesium phosphate cement, *Materials Science Forum, Trans Tech Publ* (2018) 160–167, <https://doi.org/10.4028/www.scientific.net/MSF.914.160>.
- [40] H. Ma, B. Xu, Potential to design magnesium potassium phosphate cement paste based on an optimal magnesia-to-phosphate ratio, *Mater. Des.* 118 (2017) 81–88, <https://doi.org/10.1016/j.matdes.2017.01.012>.
- [41] A.-j. Wang, J. Zhang, J.-m. Li, A.-b. Ma, L.-t. Liu, Effect of liquid-to-solid ratios on the properties of magnesium phosphate chemically bonded ceramics, *Mater. Sci. Eng. C* 33 (5) (2013) 2508–2512, <https://doi.org/10.1016/j.msec.2013.02.014>.
- [42] D.X. Li, C.H. Feng, Study on modification of the magnesium phosphate cement-based material by fly ash, *Advanced Materials Research, Trans Tech Publ* (2011) 1655–1661, [scientific.net/AMR.150-151.1655](https://doi.org/10.1016/j.amr.2011.10.1655).
- [43] B. Xu, H. Ma, H. Shao, Z. Li, B. Lothenbach, Influence of fly ash on compressive strength and micro-characteristics of magnesium potassium phosphate cement mortars, *Cement Concr. Res.* 99 (2017) 86–94, <https://doi.org/10.1016/j.cemconres.2017.05.008>.
- [44] Y. Liu, B. Chen, B. Dong, Y. Wang, F. Xing, Influence mechanisms of fly ash in magnesium ammonium phosphate cement, *Construct. Build. Mater.* 314 (2022), <https://doi.org/10.1016/j.conbuildmat.2021.125581>.
- [45] M. Aziminezhad, M. Mahdikhani, M.M. Memarpour, RSM-based modeling and optimization of self-consolidating mortar to predict acceptable ranges of rheological properties, *Construct. Build. Mater.* 189 (2018) 1200–1213.
- [46] M. Le Rouzic, T. Chaussadent, L. Stefan, M. Saillio, On the influence of Mg/P ratio on the properties and durability of magnesium potassium phosphate cement pastes, *Cement Concr. Res.* 96 (2017) 27–41, <https://doi.org/10.1016/j.cemconres.2017.02.033>.
- [47] B. Yu, J. Zhou, B. Cheng, W. Yang, Compressive strength development and microstructure of magnesium phosphate cement concrete, *Construct. Build. Mater.* 283 (2021), <https://doi.org/10.1016/j.conbuildmat.2021.122585>.